J|A|C|S
ARTICLES
Published on Web 11/09/2002

Electrogenerated Chemiluminescence 69: The Tris(2,2′-bipyridine)ruthenium(II), ($Ru(bpy)_3^{2+}$)/ Tri-*n*-propylamine (TPrA) System Revisited—A New Route Involving $TPrA^{\bullet+}$ Cation Radicals

Wujian Miao, Jai-Pil Choi, and Allen J. Bard*

Contribution from the University of Texas at Austin, Department of Chemistry & Biochemistry, Austin, Texas 78712

Received July 2, 2002

Abstract: The reaction occurring on electrooxidation of $Ru(bpy)_3^{2+}$ (bpy = 2,2′-bipyridine) and tri-*n*-propylamine (TPrA) leads to the production of $Ru(bpy)_3^{2+*}$ and light emission. The accepted mechanism of this widely used reaction involves the reaction of $Ru(bpy)_3^{3+}$ and a reduced species derived from the free radical of the TPrA. However, this mechanism does not account for many of the observed features of this reaction. A new route involving the intermediacy of TPrA cation radicals ($TPrA^{\bullet+}$) in the generation of $Ru(bpy)_3^{2+*}$ was established, based on results of scanning electrochemical microscopy (SECM)-electrogenerated chemiluminescence (ECL) experiments, as well as cyclic voltammetry simulations. A half-life of ~0.2 ms was estimated for $TPrA^{\bullet+}$ in neutral aqueous solution. Direct evidence for $TPrA^{\bullet+}$ in this medium was obtained via flow cell electron spin resonance (ESR) experiments at ~20 °C. The ESR spectra of the $TPrA^{\bullet+}$ species consisted of a relatively intense and sharp septet with a splitting of ~20 G and a *g* value of 2.0038.

Introduction

Noffsinger and Danielson[1] first reported the chemiluminescence of $Ru(bpy)_3^{3+}$ with aliphatic amines. Following this study, Leland and Powell reported the electrogenerated chemiluminescence (ECL) of the $Ru(bpy)_3^{2+}$ (bpy = 2,2′-bipyridine) with tri-*n*-propylamine (TPrA) as a coreactant.[2] Since then, a wide range of ECL analytical applications involving $Ru(bpy)_3^{2+}$ or its derivatives as labels have been reported.[3] The $Ru(bpy)_3^{2+}$ (or its derivatives) with TPrA exhibit the highest ECL efficiency, and this system forms the basis of commercial systems for immunoassay and DNA analysis.[2,3,4] The ECL intensity for this system is proportional to the concentration of both $Ru(bpy)_3^{2+}$ and TPrA species[2,4−6] and also depends on the solution pH and the electrode material.[1,2,5] The ECL mechanism of this reaction has been investigated by many workers[1,2,4,5,7] and follows the now familiar coreactant mechanism[8] where oxidation of TPrA generates a strongly reducing species. This oxidation can be via a "catalytic route" where electrogenerated $Ru(bpy)_3^{3+}$ reacts with TPrA as well as by direct reaction of TPrA at the electrode described by both Scheme 1 and Scheme 2: [where $TPrA^{\bullet+}$ = $(CH_3CH_2CH_2)_3N^{\bullet+}$, $TPrAH^+ = Pr_3NH^+$, $TPrA^{\bullet} = Pr_2NC^{\bullet}HCH_2CH_3$, $P_1 = Pr_2N^+C{=}HCH_2CH_3$, and $P_2 = Pr_2NH + CH_3CH_2CHO$]. The "catalytic" route involving homogeneous oxidation of TPrA with $Ru(bpy)_3^{3+}$ is shown in Scheme 3. The contribution of this process to the overall ECL intensity depends on the $Ru(bpy)_3^{2+}$ concentration and is small when relatively low concentrations of $Ru(bpy)_3^{2+}$ are used.[5]

Scheme 1

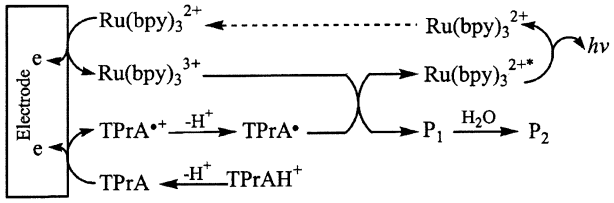

Scheme 2

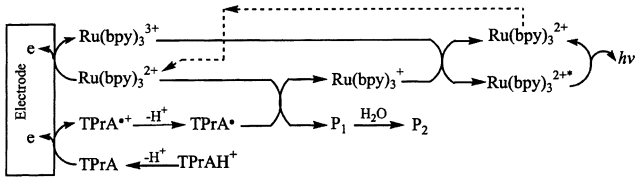

Scheme 3

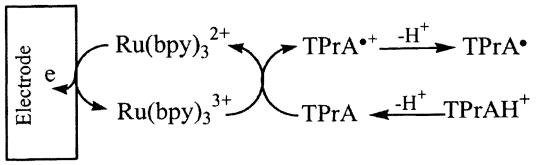

(1) Noffsinger, J. B.; Danielson, N. D. *Anal. Chem.* **1987**, *59*, 865.
(2) Leland, J. K.; Powell, M. J. *J. Electrochem. Soc.* **1990**, *137*, 3127.
(3) Bard, A. J.; Debad, J. D.; Leland, J. K.; Sigal, G. B.; Wilbur, J. L.; Wohlstadter, J. N. Chemiluminescence, Electrogenerated In *Encyclopedia of Analytical Chemistry: Applications, Theory and Instrumentation*; Meyers, R. A., Ed.; John Wiley & Sons: New York, 2000, Vol. 11, p 9842, and references therein.
(4) Kanoufi, F.; Zu, Y.; Bard, A. J. *J. Phys. Chem. B* **2001**, *105*, 210.
(5) Zu, Y.; Bard, A. J. *Anal. Chem.* **2000**, *72*, 3223.
(6) Gross, E. M.; Pastore, P.; Wightman, R. M. *J. Phys. Chem. B* **2001**, *105*, 8732.
(7) He, L.; Cox, K. A.; Danielson, N. D. *Anal. Lett.* **1990**, *23*, 195.
(8) Rubinstein, I.; Bard, A. J. *J. Am. Chem. Soc.* **1981**, *103*, 512.

10.1021/ja027532v CCC: $22.00 **© 2002 American Chemical Society**

The mechanisms proposed above, however, do not account for a number of observations made for this ECL system. The strong dependence of ECL efficiency on electrode material[5] and surfactants[9−12] strongly supports the importance of the direct oxidation of TPrA. However, two ECL waves occur at a glassy carbon and a gold electrode, with the first ECL wave in a potential range less positive than that for the oxidation of $Ru(bpy)_3^{2+}$ (whereas the second wave occurs at potentials for $Ru(bpy)_3^{2+}$ oxidation). Both waves were associated with the emission of $Ru(bpy)_3^{2+*}$ to $Ru(bpy)_3^{2+}$. The necessary oxidant to produce ECL at this first wave is not apparent. Moreover, in the commercial Origen analyzer (IGEN International, Inc., Gaithersburg, MD), the $Ru(bpy)_3^{2+}$-tagged species in an immunoassay are immobilized on 2.8 μm diameter magnetic beads that are brought to an electrode by a magnetic field. Direct oxidation of $Ru(bpy)_3^{2+}$ on the beads would only occur for those within electron tunneling distance from the electrode, ~1 to 2 nm, so most of the labels on the bead would not contribute to the ECL response. However, the high sensitivity of the technique indicates that most of the labels on the beads participate in the reaction, so that some other reactions involving the TPrA coreactant must generate precursors that can form $Ru(bpy)_3^{2+*}$. Clearly, the present ECL mechanisms proposed above (Schemes 1−3) cannot explain these results. Moreover, there has been no convincing explanation of the relative efficiencies of related coreactants, e.g., Et_3N vs TPrA, based on the mechanism that only involves the free radical reductant as an intermediate (e.g., correlating the reducing power of the radical with observed ECL emission efficiency). Studies that attempting to correlate coreactant efficiency with electron donating/withdrawing power of the amine have been reported previously.[13]

An understanding of the mechanism of the $Ru(bpy)_3^{2+}$/TPrA system is important in designing and selecting new coreactants and in improving the sensitivity and reproducibility of the ECL system. In this paper, a new route involving $TPrA^{\bullet+}$ cation radical reduction for the generation of the excited-state $Ru(bpy)_3^{2+*}$ is presented. This mechanism is supported by a scanning electrochemical microscopy (SECM)−ECL experiment, cyclic voltammetry (CV), and CV digital simulations, and by the direct detection by electron spin resonance (ESR) showing that the $TPrA^{\bullet+}$ cation radical is relatively stable under conditions similar to those used in the ECL experiments, i.e., in aqueous solutions at neutral pH.

Experimental Section

Chemicals. Tris(2,2′-bipyridyl)ruthenium(II) dichloride hexahydrate ($Ru(bpy)_3Cl_2 \cdot 6H_2O$), tri-*n*-propylamine (TPrA, 99+ %), and Fremy's salt [$(KSO_3)_2NO$] from Aldrich (Milwaukee, WI), (3-aminopropyl)-trimethoxysilane [$(CH_3O)_3Si(CH_2)_3NH_2$, ≥ 97%] and lithium perchlorate ($LiClO_4$, > 99%) from Fluka (Milwaukee,WI), potassium permanganate ($KMnO_4$), sodium phosphate dibasic heptahydrate ($Na_2HPO_4 \cdot 7H_2O$, 98.0%), and phosphoric acid (H_3PO_4, 85%) from Fisher (Fairlawn, NJ), potassium phosphate monobasic (KH_2PO_4, 99.6%) from J. T. Baker (Phillipsburg, NJ), tris(hydroxymethyl)aminomethane (Tris, ultrapure) from Life Technologies (Rockville, MD), 1-ethyl-3-(3-dimethylaminopropyl) carbodiimide hydrochloride (EDAC, SigmaUltra) and 1-methylimidazole from Sigma (St. Louis, MO), hydrochloric acid (HCl, GR) from EM (Gibbstown, NJ), toluene (A. R.) from Mallinckrodt (Hazelwood, MO), and EtOH (200-proof) from Aaper Alcohol (Shelbyville, KY) were used without further purification. Bis(2,2′-bipyridine)-4,4′-dicarboxy-2,2′-bipyridineruthenium(II) hexa- fluorophosphates $\{Ru(bpy)_2[bpy(COOH)_2](PF_6)_2\}$ was prepared by following a procedure in the literature.[14] Unless otherwise stated, all solutions were freshly prepared with deionized water (Milli Q, Millipore).

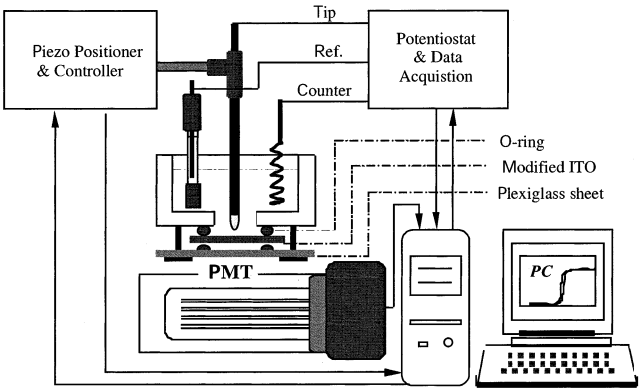

Figure 1. Setup for SECM−ECL.

Immobilization of $Ru(bpy)_2[bpy(COOH)_2]^{2+}$ on an ITO Electrode. A clean, dried indium tin oxide (ITO) electrode (resistance, 30−60 ohm/square; Delta Technologies, Stillwater, MN) with dimensions of ~1 × 1 cm was immersed in a 5% of $(CH_3O)_3Si(CH_2)_3NH_2$ toluene solution and kept in a desiccator for 24 h. During this process, $(CH_3O)_3Si(CH_2)_3NH_2$ becomes immobilized by formation of ITO/O−$Si(CH_2)_3NH_2$ bonds.[15] The electrode was then washed with EtOH and transferred into a 0.10 M 1-methylimidazole/HCl buffer solution (pH = 7) containing ~10 mM $Ru(bpy)_2[bpy(COOH)_2]^{2+}$ and 10 mM EDAC. After a 45 min incubation at 70 °C, the ITO electrode was washed thoroughly with EtOH and then water. By this treatment, a layer of $Ru(bpy)_2[bpy(COOH)_2]^{2+}$ was covalently attached to the aminosilane formed previously on the ITO, to produce ITO/O−$Si(CH_2)_3NH$−[CO-(bpy)(COOH)](bpy)$_2$Ru(II) (designated as ITO/OSiRu^{II}). The ITO/OSiRu^{II} electrode was subsequently immersed in a 0.10 M Tris/HCl buffer (pH = 8) and maintained in the dark until further use.

Electrochemical and ECL Measurements. Fast scan CV was performed with the model 660 electrochemical workstation (CH Instruments, Austin, TX). A conventional three-electrode cell was used, with a Pt wire as the counter electrode and an Ag/AgCl/KCl(sat.) as the reference electrode. The working electrodes used for the examination of TPrA redox behavior at fast scan rates were of different materials [Pt, Au, carbon fiber, and glassy carbon (GC)] and different dimensions (3 mm, 100 μm, 25 μm, 5 μm diameter Pt; 2 mm diameter Au; 3 mm diameter GC and 10 μm diameter carbon fiber). The ECL along with the CV signals were measured simultaneously with a home-built potentiostat combined with a photomultiplier tube (PMT, Hamamatsu R4220p, Japan) installed under the electrochemical cell. A voltage of −750 V was supplied to the PMT with a high-voltage power supply series 225 (Bertan High Voltage Corp., Hicksville, NY). A 3 mm diameter GC working electrode, and the counter and reference electrodes the same as those used for fast scan CV were used.

The SECM-ECL experiments were taken with a CHI 900 SECM system (CH Instruments, Austin, TX) combined with the ECL instrument described. Figure 1 shows a schematic diagram of the setup. The working electrode (tip), was a 1.5 mm diameter hemispherical Au, and the ITO/OSiRu^{II} ("modified ITO") served as the substrate. The direct oxidation of covalently attached $Ru(bpy)_2[bpy(COOH)_2]^{2+}$ species at

(9) Zu, Y.; Bard, A. J. *Anal. Chem.* **2001**, *73*, 3960.
(10) McCord, P. M.; Bard, A. J. *J. Electroanal. Chem.* **1991**, *318*, 91.
(11) Factor, B.; Muegge, B.; Workman, S.; Boltan, E.; Bos, J.; Richter, M. M. *Anal. Chem.* **2001**, *173*, 4621, and references therein.
(12) Bruce, D.; McCall, J.; Richter, M. M. *Analyst* **2002**, *127*, 125.
(13) Knight, A. W.; Greenway, G. M. *Analyst* **1996**, *121*, 101R.
(14) Sprintschnik, G.; Sprintschnik, H. W.; Kirsch, P. P.; Whitten, D. G. *J. Am. Chem. Soc.* **1977**, *99*, 4947.
(15) Murray, R. W. In *Electroanalytical Chemistry*; Bard, A. J., Ed.; Marcel Dekker: New York, 1984; Vol. 13, p 191.

the ITO electrode was avoided by holding the electrode at an open circuit. A Pt wire and an Ag/AgCl/KCl (sat.) electrode were also used as the counter and reference electrodes, respectively.

The simulation of the cyclic voltammogram of TPrA oxidation in aqueous solution was carried out by using the simulation package DigiSim V 3.03 (Bioanalytical Systems Inc., West Lafayette, IN).

ESR Experiments. The cation radical of TPrA, $TPrA^{\bullet+}$, was generated by flowing 0.10 M TPrA (pH 7, adjusted by HNO_3) and ~0.03 M $Ru(bpy)_3^{3+}$ solutions through a quartz flat cell[16] via a two-jet mixing chamber (Wilmad, Prod. No. WG-801-Q, Buena, NJ). The $Ru(bpy)_3^{3+}$ solution was freshly prepared by bubbling Cl_2 gas, generated via the reaction of solid $KMnO_4$ and concentrated HCl, directly into a 0.030 M $Ru(bpy)_3Cl_2$ solution. A clear color change from reddish orange to dark greenish blue was observed upon the complete oxidation of $Ru(bpy)_3^{2+}$ to $Ru(bpy)_3^{3+}$.

X-band ESR spectra were recorded on an ER-300 ESR spectrometer (IBM Instruments Inc.) with a modulation frequency of 100 kHz and microwave power at 12.6 mW. The swept field and the *g* value were calibrated externally using a 5.0 mM aqueous Fremy's salt solution.[17,18] The quartz flat cell was installed in a TE_{102} rectangular cavity. Overall, solution flow rates of 2−5 mL/s were employed, and the relative flow rates for the TPrA and $Ru(bpy)_3^{3+}$ solutions were adjusted so that an orange color appeared at the outlet of the flow cell.

The spectra were simulated using PEST Winsim Software[19] (National Institute of Environmental Health Sciences, National Institute of Health, Research Triangle Park, NC).

All experiments were conducted at a temperature of 20 ± 2 °C, unless otherwise stated.

Results and Discussion

Electrochemical and ECL Behavior of the $Ru(bpy)_3^{2+}$/TPrA System. An earlier report[5] showed that at low concentrations of $Ru(bpy)_3^{2+}$ (~μM) and 10−100 mM TPrA in aqueous 0.15 M phosphate buffer, pH 7.5, the ECL emission vs potential curves displayed two broad waves. Similar behavior was also observed in the presence of 0.10 M TPrA when a much lower concentration of $Ru(bpy)_3^{2+}$, 1.0 nM, (Figure 2a) and a different buffer solution, 0.10 M Tris/0.10 M $LiClO_4$, pH = 8, were used (Figure 2). The initial ECL signal started at potentials where the direct oxidation of TPrA at the GC electrode occurs (Figure 2a,b), and reached a first maximum at a potential of about 0.90 V vs Ag/AgCl, about 50 mV less positive than the peak potential for TPrA oxidation, and well before $Ru(bpy)_3^{2+}$ oxidation. The second ECL signal has a peak potential value of 1.14 V vs Ag/AgCl, in the potential region of the direct oxidation of $Ru(bpy)_3^{2+}$ at a GC electrode.[5] For comparison, Figure 2 also includes the ECL signal profile obtained with the $Ru(bpy)_3^{2+}$ concentration of 1.0 μM (Figure 2c). The corresponding TPrA oxidation CV is not included because it is essentially the same as that in Figure 2b. The relative ECL intensity from the first wave is significant, particularly in the 1.0 nM $Ru(bpy)_3^{2+}$ solution, and thus, the bulk of the ECL signal obtained in this system with low concentrations of analytes, as in immunoassays and DNA probes with $Ru(bpy)_3^{2+}$ as an ECL label, probably originates from the first ECL wave.

Note that even with a high concentration of $Ru(bpy)_3^{2+}$ (~mM), the ECL signal first appeared in a potential range less positive than that for the oxidation of $Ru(bpy)_3^{2+}$. However, the initial ECL signal is relatively small compared to the large

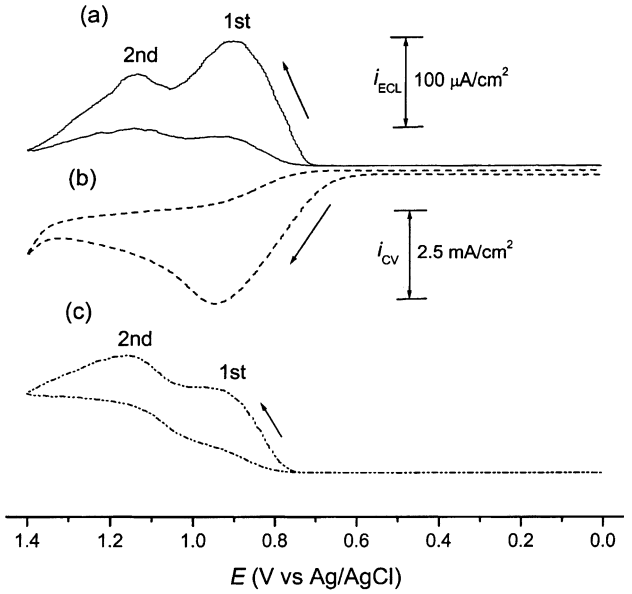

Figure 2. (a) ECL and (b) cyclic voltammogram of 1.0 nM $Ru(bpy)_3^{2+}$ in the presence of 0.10 M TPrA with 0.10 M Tris/0.10 M $LiClO_4$ buffer (pH = 8) at a 3 mm diameter glassy carbon electrode at a scan rate of 50 mV/s. (c) As (a) but with 1.0 μM $Ru(bpy)_3^{2+}$. The ECL intensity scale is given for (c) and should be multiplied by 100 for (a).

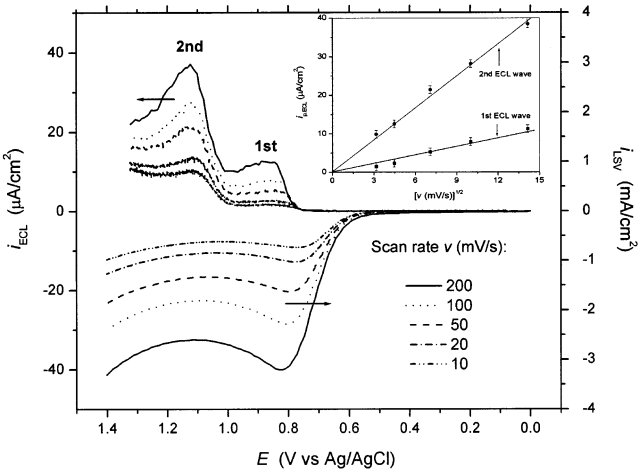

Figure 3. Linear sweep voltammograms and their corresponding ECL signals for 1 μM $Ru(bpy)_3^{2+}$ and 50 mM TPrA in pH 8.5 PBS at a 3 mm diameter glassy carbon electrode at different scan rates. Inset, plot of the first and the second ECL signals versus $v^{1/2}$.

ECL signal generated via Schemes 1 and 2. Note also that the ECL signal observed under current conditions is not due to the reaction of $Ru(bpy)_3^{2+}$ with hydroxide in solution as reported previously[20] because no ECL signal was seen in the absence of TPrA when the electrode potential was scanned from 0 to 1. 4 V vs Ag/AgCl for the oxidation of $Ru(bpy)_3^{2+}$ in a buffer solution of 0.10 M Tris/0.10 M $LiClO_4$, pH = 8.

Figure 3 shows linear sweep voltammograms and the corresponding ECL signals obtained from 1 μM $Ru(bpy)_3^{2+}$ and 50 mM TPrA in 0.20 M phosphate buffer solution (PBS, pH 7.5) at a GC electrode at different potential scan rates (v). A linear relationship between the ECL peak intensity ($i_{p,ECL}$) for both the first and the second ECL waves and $v^{1/2}$ was observed (Figure 3, inset), consistent with the linear relationship between the peak current for the oxidation of TPrA and $v^{1/2}$. These results

(16) Charkoudian, J. C. *J. Magn. Reson.* **1984**, *57*, 287.
(17) Windle, J. J.; Wiersema, A. K. *J. Chem. Phys.* **1963**, *39*, 1139.
(18) Pake, G. E.; Townsend, J.; Weissman, S. I. *Phys. Rev.* **1952**, *85*, 682.
(19) Duling, D. R. *J. Magn. Reson., Ser. B* **1994**, *104*, 105.
(20) Hercules, D. M.; Lytle, F. E. *J. Am. Chem. Soc.* **1996**, *88*, 4745.

suggest that under current experimental conditions, both the first and the second ECL signals are directly related to the oxidation of TPrA.

The effect of both TPrA and $Ru(bpy)_3^{2+}$ concentrations on the first ECL peak intensity ($i_{p1,ECL}$) was also investigated. As shown in Figure 4a, in 1 μM $Ru(bpy)_3^{2+}$ (0.20 M PBS, pH 7.5), the $i_{p1,ECL}$ is linearly proportional to the concentration of TPrA. No ECL signal was detected in the absence of either TPrA or $Ru(bpy)_3^{2+}$, so the first ECL signal must be associated with a reaction between the species generated from TPrA and $Ru(bpy)_3^{2+}$. Figure 4b shows the $i_{p1,ECL}$ changes as a function of $Ru(bpy)_3^{2+}$ concentration when TPrA concentration kept at a constant value of 100 mM (0.20 M PBS, pH 8.5). In the range of 10 pM to 50 μM of $Ru(bpy)_3^{2+}$, $i_{p1,ECL}$ steadily rises with an increase of $Ru(bpy)_3^{2+}$ concentration. Beyond 50 μM, $i_{p1,ECL}$ reaches a plateau. In contrast, the ECL intensity of the second wave was always proportional to the concentration of $Ru(bpy)_3^{2+}$, for concentrations up to 1 mM. Figure 4c shows both the first and the second ECL responses when the $Ru(bpy)_3^{2+}$ concentration was in the "plateau" range of 50 μM to 1.0 mM. These results clearly indicate that the mechanism for the first ECL signal is different from the second one. As demonstrated later, the intensity of the first ECL signal is determined by the quantity of TPrA derived radicals (cation and free) generated from the oxidation of TPrA at the electrode. In a relative excess of $Ru(bpy)_3^{2+}$ solution, the $i_{p1,ECL}$ is governed by the concentration of TPrA (Figure 4a). On the other hand, when the reaction produces excess TPrA radicals relative to the concentration of $Ru(bpy)_3^{2+}$, the $i_{p1,ECL}$ will be controlled by the concentration of $Ru(bpy)_3^{2+}$. When the $Ru(bpy)_3^{2+}$ concentration is equivalent to or greater than the concentration of radicals formed from TPrA oxidation, the $i_{p1,ECL}$ will be independent of the concentration of $Ru(bpy)_3^{2+}$. Figure 4c exhibits these two features simultaneously. Studies on the relationship between $i_{p2,ECL}$ and TPrA concentration have been reported previously.[2,5,6]

SECM−ECL Experiments. To prove that oxidation of TPrA generates an ECL signal without direct oxidation of $Ru(bpy)_3^{2+}$, experiments with the instrumental setup shown in Figure 1 were carried out. In this experiment, $Ru(bpy)_2[bpy(COOH)_2]^{2+}$, whose ECL behavior is very similar to that for $Ru(bpy)_3^{2+}$ in the presence of TPrA,[12] was covalently immobilized on an ITO electrode. During the course of the SECM−ECL experiment, this modified ITO electrode was at an open circuit potential and served as the substrate. The reaction medium used was 10.0 mM TPrA solution in 0.10 M Tris/0.10 M $LiClO_4$ buffer (pH = 8). Note that the tip in this experiment was considerably larger than those usually employed in SECM[21] to generate a sufficient flux of TPrA radicals to obtain an observable emission signal. However, this electrode still showed a decreasing SECM current response on approach to a substrate that blocked diffusion of reactant to the tip (Figure 5). The distance between the tip and the substrate (d) was estimated from this approach curve. By holding the tip potential at 0.85 V vs Ag/AgCl, where TPrA oxidation occurs, a gradual decrease in tip current was initially observed as the tip slowly approached the substrate (~0.05 μm/s at the last stage). The zero distance was indicated by a sudden increase in the tip current when contact is made between the tip and ITO. The tip was withdrawn from the substrate a given distance and cycled between 0 and 1.0 V vs Ag/AgCl at υ = 50 mV/s, and the current and any ECL signal generated in the electrochemical cell were monitored. A typical experimental result for $d = -1.92$ μm is given in Figure 6.

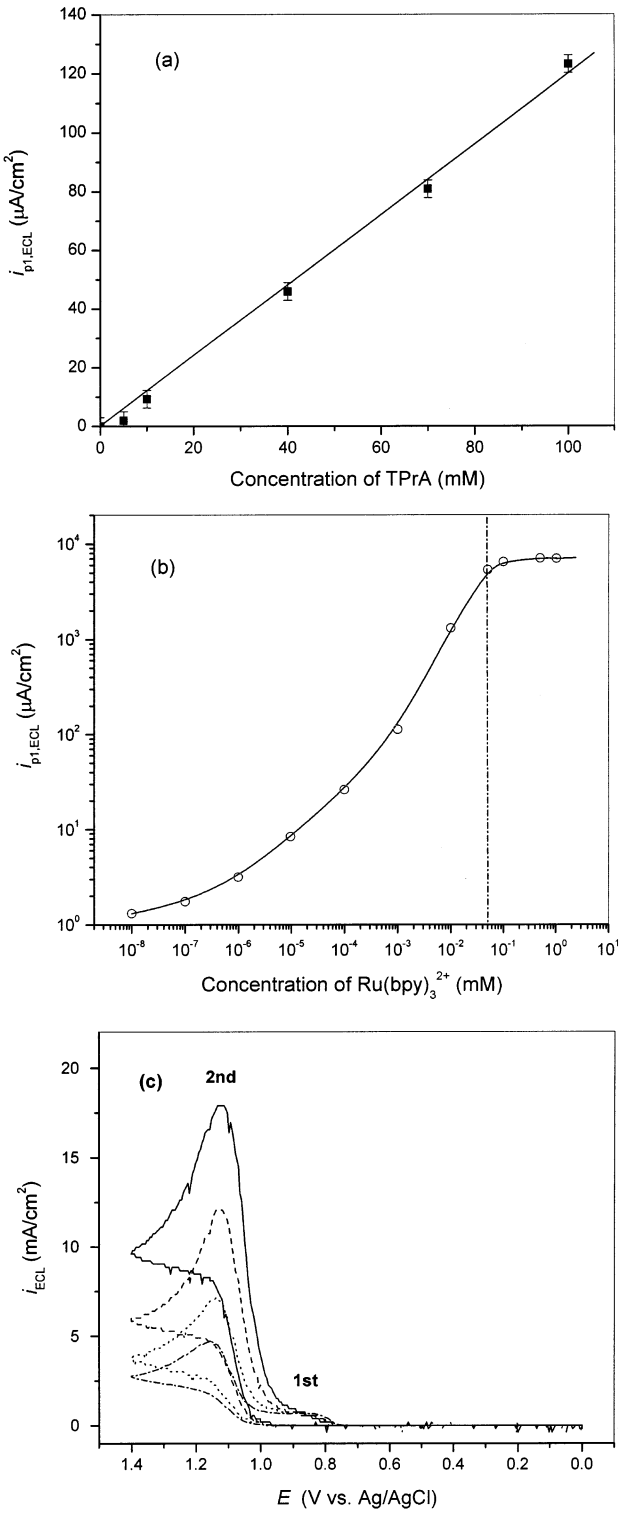

Figure 4. (a) First ECL peak intensity as a function of TPrA concentration with 1 μM $Ru(bpy)_3^{2+}$ (0.20 M PBS, pH 7.5). (b) The first ECL peak intensity as a function of $Ru(bpy)_3^{2+}$ concentration with 100 mM TPrA (0.20 M PBS, pH 8.5). (c) The first and the second ECL responses in 100 mM TPrA (0.20 M PBS, pH 8.5) with different $Ru(bpy)_3^{2+}$ concentrations: 1 mM (solid line), 0.50 mM (dashed line), 0.10 mM (dotted line) and 0.05 mM (dash−dotted line). A 3 mm diameter glassy carbon electrode was used at a scan rate of 100 mV/s.

(21) Bard, A. J., Mirkin, M. V., Eds. *Scanning Electrochemical Microscopy*; Marcel Dekker: New York, 2001,

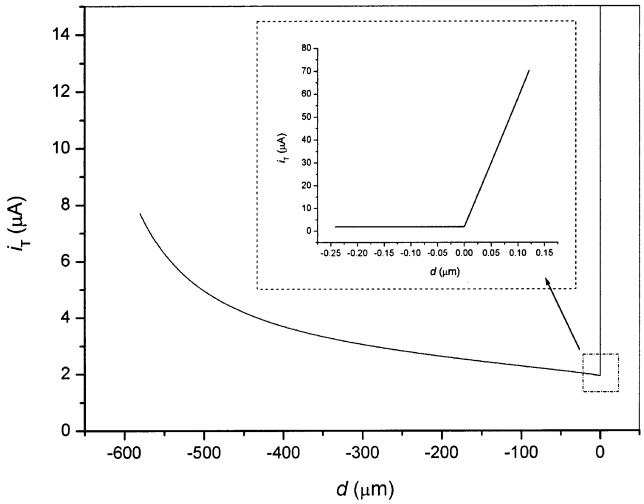

Figure 5. Approach curve obtained for the oxidation of 10.0 mM TPrA (0.10 M Tris/0.10 M $LiClO_4$ buffer, pH = 8) at a 1.5 mm diameter hemispherical Au electrode held at 0.85 V vs Ag/AgCl. An ITO/OSiRu^{II} electrode at open circuit served as the substrate. The detailed i_T vs d profile around $d = 0$ is shown in the inset.

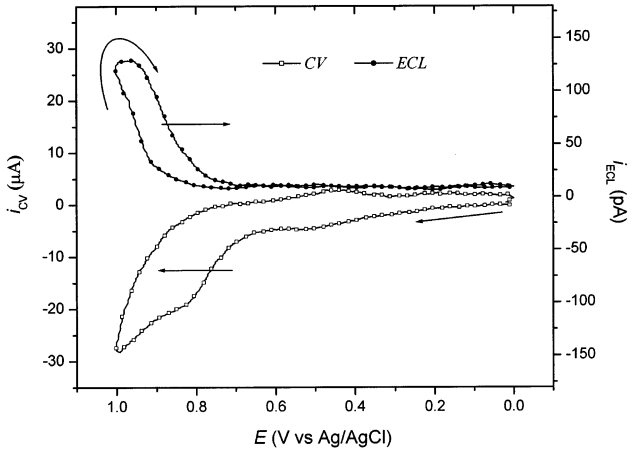

Figure 6. Cyclic voltammogram and ECL signal obtained in 10.0 mM TPrA (0.10 M Tris/0.10 M $LiClO_4$ buffer, pH = 8) at a 1.5 mm diameter hemispherical Au electrode when the tip/substrate separation distance, d,was 1.92 μm. A scan rate of 50 mV/s was used, and the substrate was an ITO/OSiRu^{II} electrode at open circuit.

Upon oxidation of TPrA at ~0.80 V vs Ag/AgCl, an ECL signal appears and tracks the tip current during potential cycling. A pair of prewaves located at ~0.5 V vs Ag/AgCl on the CV were frequently observed during the oxidation of TPrA, and may be attributed to the gold surface oxide formation and reduction.[5] The ECL signal could be detected only within a very small d (< ~5−6 μm); the maximum intensity as a function of the tip distance is shown in Figure 7. At short distance, the ECL intensity decreased almost exponentially with the tip distance, indicating that the amount of dissolved $Ru(bpy)_2[(bpy(COOH)_2)]^{2+}$ species from the substrate in the solution phase (if any) is negligible under the experimental conditions. This experiment clearly demonstrates that by simply oxidizing TPrA intermediates are formed that can cause excitation of $Ru(bpy)_3^{2+}$ and is a direct confirmation of the ability to form excited states at all positions of a 2.8 μm bead on an electrode surface.

The electrochemical oxidation of TPrA under various conditions has been extensively studied and the following mechanism for reactions occurring in aqueous solution is generally accepted

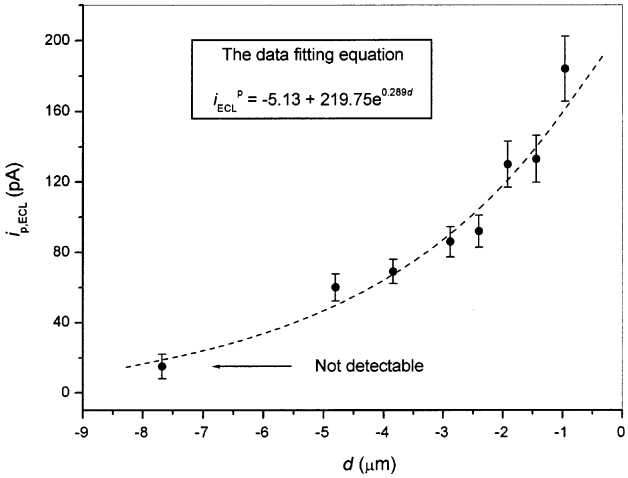

Figure 7. ECL peak intensity as a function of tip distance.

Scheme 4

$$TPrAH^+ \overset{pK_a = 10.4}{\rightleftharpoons} TPrA + H^+ \quad (4.1)$$

$$TPrA \xrightarrow{k_s} TPrA^{\bullet+} + e \quad (4.2)$$

$$TPrA^{\bullet+} \underset{k_b}{\overset{k_f}{\rightleftharpoons}} TPrA^{\bullet} + H^+ \quad (4.3)$$

$$TPrA^{\bullet} \xrightarrow{k_s} P1 + e \quad (4.4)$$

$$P1 + H_2O = P2 \quad (4.5)$$

$$\text{and} \quad TPrA^{\bullet+} + TPrA^{\bullet} = TPrA + P1 \quad (4.6)$$

(Scheme 4):[4,22−26] (where $TPrA^{\bullet+}$, TPrA, P1, and P2 species have the same significance as in Scheme 2).

Deprotonated TPrA molecules first undergo one-electron oxidation to form TPrA cation radicals ($TPrA^{\bullet+}$), which rapidly deprotonate to form TPrA free radicals ($TPrA^{\bullet}$). These oxidize further by losing one electron to produce the iminium ion (P1), which subsequently hydrolyzes to products, P2.

On the basis of previous study,[5] we believe that the ECL signal generated under the present conditions is the emission of immobilized $Ru(bpy)_2[(bpy(COOH)_2)]^{2+*}$, simplified as "$Ru(bpy)_3^{2+*}$ in the following discussions because $Ru(bpy)_2[(bpy(COOH)_2)]^{2+}$ and $Ru(bpy)_3^{2+}$ species exhibit very similar electrochemical[27] and ECL[12] behavior. According to Scheme 4, the direct oxidation of TPrA at the tip of SECM − ECL experiments leads to the formation of reducing radicals ($TPrA^{\bullet}$, $E° \approx -1.7$ V vs Ag/AgCl[28]) that can diffuse away from the tip and reach the substrate and react with immobilized $Ru(bpy)_3^{2+}$ to generate $Ru(bpy)_3^{+}$. To produce $Ru(bpy)_3^{2+*}$, some oxidant is required to remove an electron from $Ru(bpy)_3^{+}$. The most likely oxidant candidate in this system is the cation radical $TPrA^{\bullet+}$, $E° \approx 0.83$ to 0.95 V vs Ag/AgCl. However, the deprotonation process of $TPrA^{\bullet+}$ to $TPrA^{\bullet}$ has usually been taken to be an extremely rapid process, resulting in an insufficient flux of $TPrA^{\bullet+}$ from the tip to produce measurable ECL. We considered the possible production of $Ru(bpy)_3^{3+}$ from reaction of $Ru(bpy)_3^{2+}$ with $TPrA^{\bullet+}$, but the redox potential of the $TPrA^{\bullet+}$/TPrA couple is not sufficient for this reaction (see

(22) Chow, Y. L.; Danen, W. C.; Nelsen, S. F.; Rosenblatt, D. H. *Chem. Rev.* **1978**, *78*, 243.
(23) Mann, C. K. *Anal. Chem.* **1964**, *36*, 2424.
(24) Masui, M.; Sayo, H.; Tsuda, Y. *J. Chem. Soc., B* **1968**, 973.
(25) Portis, L. C.; Bhat, V. V.; Mann, C. K. *J. Org. Chem.* **1970**, *35*, 2175.
(26) Ross, S. D. *Tetrahedron Lett.* **1973**, 1237.
(27) Elliott, C. M.; Hershenhart, E. J. *J. Am. Chem. Soc.* **1982**, *104*, 7519.

Scheme 5

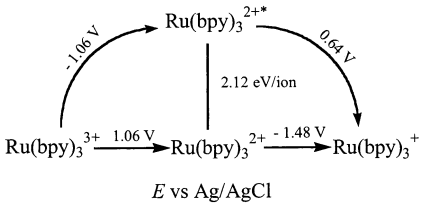

Scheme 6

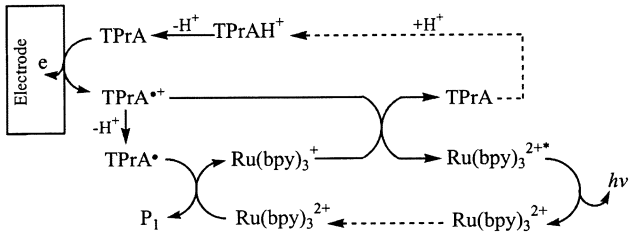

Scheme 5,[29] where the potentials have been converted to Ag/AgCl by taking $E^0_{Ag/AgCl} = 0.20$ V vs NHE[30]).

Scheme 6 summarizes a new route for the generation of ECL within the potential range before direct oxidation of $Ru(bpy)_3^{2+}$ at the electrode, involving formation of excited state on reaction of $TPrA^{\bullet+}$ with $Ru(bpy)_3^{+}$ (formed by reaction of $Ru(bpy)_3^{2+}$ with $TPrA^{\bullet}$).

If the maximum distance at which light is observed, ~6 μm, represents the distance that $TPrA^{\bullet+}$ can diffuse before deprotonation, given a typical diffusion coefficient of 5×10^{-6} cm^2/s, the half-life, $\tau_{1/2}$, of the cation radical would be ~0.2 ms (See the next section for details). A similar lifetime of the $TPrA^{\bullet+}$ can also be inferred from the data in ref 6.

Fast Scan CV and Digital Simulations. With $\tau_{1/2} \approx 0.2$ ms, one would estimate that $TPrA^{\bullet+}$ could be detected by CV, if $\upsilon >$ ~130 V/s (~$RT/F\tau_{1/2}$).[30] Fast scan CV experiments were thus carried out to detect $TPrA^{\bullet+}$ species after TPrA oxidation at the electrode by scan reversal. A wide range of TPrA aqueous solutions (~0.010 to 0.10 M) with different supporting electrolytes and different pHs (from 0.2 M H_2SO_4 to pH ≈ 10), different materials of the working electrode (GC, carbon fiber, Au, Pt) with different dimensions (from 5 μm to 3 mm diameters), and different scan rates between 20 mV/s and 1000 V/s were used. However, no wave associated with the reduction of $TPrA^{\bullet+}$ on the reverse scan of the CVs was ever found. Scan rates faster than 1000 V/s and CV with background subtraction were also tried without success, since in these cases, significant charging currents and probably limitations from the rate of the heterogeneous electron transfer from TPrA interfered.

The failure to detect the cation radical can be ascribed to the fact that the oxidation of TPrA is an ECE process[30] and that at potentials where $TPrA^{\bullet+}$ is reduced, the radical $TPrA^{\bullet}$ is oxidized, so that a cathodic current is at least partially compensated by an anodic one. To investigate this effect, CV digital simulations following Scheme 4 were carried out assuming different values for the heterogeneous electron-transfer rate constants [k_s in eqs 4.1 and 4.4], and the k_f and k_b values of eq 4.3. Other parameters were either adopted from the literature or assigned to reasonable values. Figure 8a shows a simulated

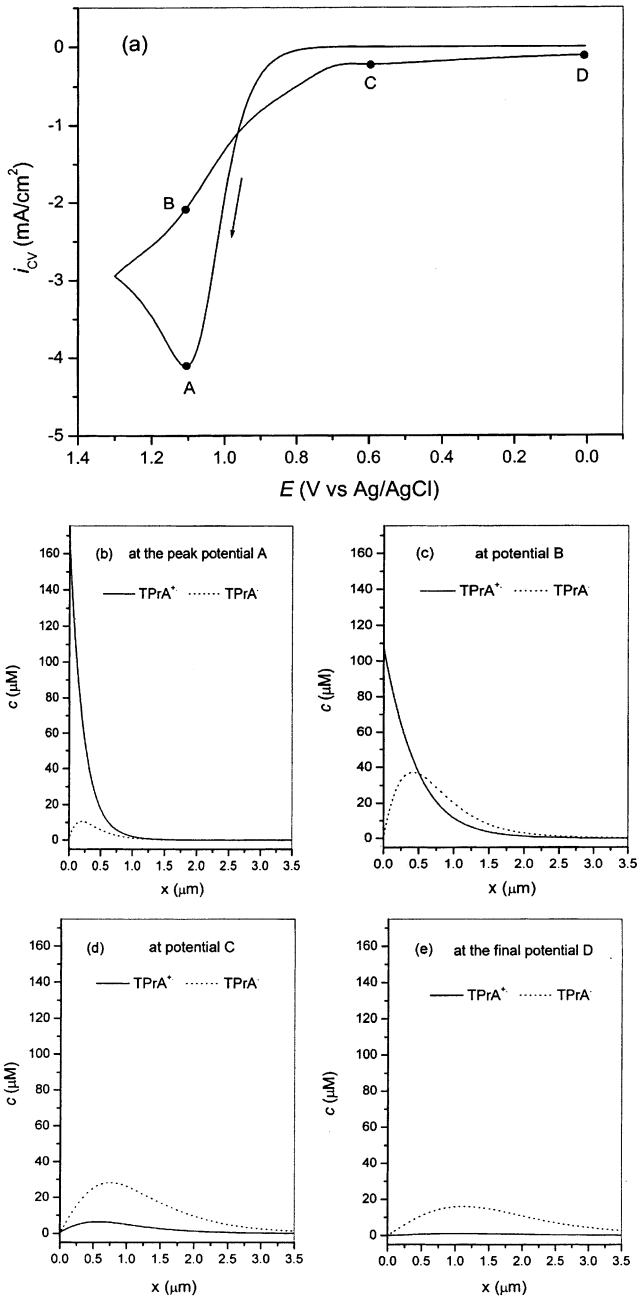

Figure 8. (a) A simulated CV of TPrA oxidation in pH 8 solution at a scan rate of 900 V/s. (b) to (e) The concentration profiles for $TPrA^{\bullet+}$ (solid line) and $TPrA^{\bullet}$ (dotted line) at a specific points, A, B, C, and D, shown in (a). Parameters used in the simulation were (see Scheme 4 for further information): $E^0_{TPrA^{\bullet+}/TPrA} = 0.88$ V vs Ag/AgCl, k_s (for eqs 4.2 & 4.4) = 0.01 cm/s, $E^0_{P1/TPrA^{\bullet}} = -1.7$ V vs Ag/AgCl, for eq 4.3 $k_f = 3500$ s^{-1} & $k_b = 7 \times 10^6$ s^{-1}, $c_{(TPrA+TPrAH+)} = 10$ mM. All species were assumed to have a diffusion coefficient of 5×10^{-6} cm^2/s except for H^+ ($D_{H+} = 5 \times 10^{-5}$ cm^2/s).

CV of TPrA oxidation in pH 8 solution at a scan rate of 900 V/s, with the parameters shown in the figure caption. The cross over on the reverse scan, where the anodic current is larger on the reverse scan than it is on the forward scan current (at ~0.96 V vs Ag/AgCl), can be attributed to the greater contribution of $TPrA^{\bullet}$ to the measured current. The concentration profiles (c vs x) for both $TPrA^{\bullet+}$ and $TPrA^{\bullet}$ at specific potential values are shown in Figure 8b−e. Upon the oxidation of TPrA, a significant amount of $TPrA^{\bullet+}$ cation radical is formed at the electrode surface (Figure 8b), which further dissociated to $TPrA^{\bullet}$.

(28) Lai, R., Bard, A. J., unpublished experiments.
(29) Roundhill, D. M. In *Photochemistry and Photophysics of Metal Complexes*; Fackler, J. J. P., Ed.; Plenum Press: New York, 1994; p 165.
(30) Bard, A. J.; Faulkner, L. R. *Electrochemical Methods*; 2nd ed.; John Wiley & Sons. Inc.: New York, 2000.

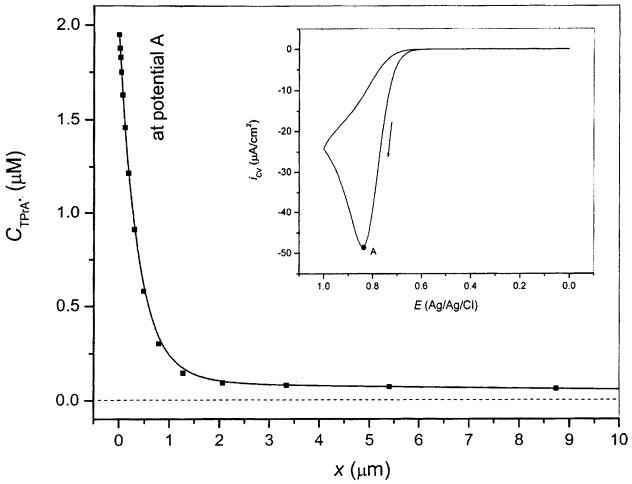

Figure 9. Simulated concentration profile for $TPrA^{\bullet+}$ formed at a 1.5 mm diameter hemispherical tip. This curve corresponds to potential A on the cyclic voltammogram (inset) for 10.0 mM TPrA (0.10 M Tris/0.10 M $LiClO_4$, pH 8) with a scan rate of 50 mV/s. Other parameters required for the simulation are as in Figure 8.

Because the free radical is a very strong reducing agent and can be oxidized immediately at the electrode, its surface concentration equaling zero is expected. During the potential scan period of A to B (Figure 8b−c), due to the continuous conversion of $TPrA^{\bullet+}$ to $TPrA^{\bullet}$, as well as diffusion to the bulk solution, the surface concentration of $TPrA^{\bullet+}$ starts to decrease, while the overall amount of $TPrA^{\bullet}$ in the electrode surface region increases. After potential B, substantial reduction of $TPrA^{\bullet+}$ to TPrA is expected, which results in a cathodic current and the surface concentration of $TPrA^{\bullet+}$ species decreases dramatically (Figure 8d). Note that even in this potential region, the overall current at the electrode is always anodic, because the current contribution from the oxidation of $TPrA^{\bullet}$ is larger. Therefore, the absence of a reduction wave following the oxidation of TPrA with fast scan CV does not indicate that $TPrA^{\bullet+}$ is so unstable that it cannot participate in the ECL reaction.

These digital simulations were also carried out to evaluate the lifetime of $TPrA^{\bullet+}$ based on the data obtained from the previous SECM−ECL experiment in 10 mM TPrA (pH 8). Figure 9 shows the simulated concentration distribution for $TPrA^{\bullet+}$ formed at the tip as a function of distance from the tip. This curve was recorded at the potential A on the CV (inset of Figure 9), at which a maximum surface concentration and a maximum diffusion distance of $TPrA^{\bullet+}$ were observed. By comparing the data shown in Figure 9 with those in Figure 7, about 3.6% of the initial $TPrA^{\bullet+}$ (or 71 nM, at $x = 6\ \mu$m, Figure 9) are needed to diffuse to the substrate and react with immobilized $Ru(bpy)_3^{2+}$ to generate an ECL signal.

With the assumption that the $TPrA^{\bullet+}$ deprotonation reaction (eq 4.3) is a first-order process, the half-life ($\tau_{1/2}$) of $TPrA^{\bullet+}$ is $\tau_{1/2} = 0.693/k_f$, where k_f is the forward rate constant of eq 4.3, $\sim$3500 s^{-1} based on the digital simulation. Thus, $\tau_{1/2} \sim 0.2$ ms for $TPrA^{\bullet+}$ cation radicals can be estimated.

ESR of $TPrA^{\bullet+}$ in Aqueous Solution. With the above estimated lifetime, it should be possible to detect $TPrA^{\bullet+}$ by ESR. Tertiary amine radical cations are generally believed to be short-lived intermediates in amine oxidation because of rapid deprotonation at the α-carbon to produce α-aminoalkyl free radicals.[22,31] However, previous studies also have shown that trimethylamine radical cation has a similar lifetime as that

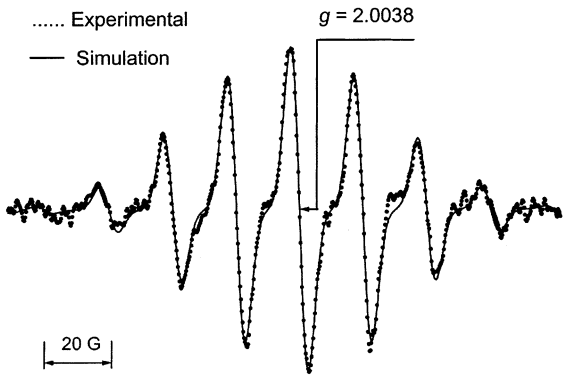

Figure 10. Experimentally measured (dotted line) and simulated (solid line) ESR spectra of $TPrA^{\bullet+}$ generated by the oxidation of TPrA by $Ru(bpy)_3^{3+}$ in an aqueous pH 7 solution at 20 °C.

estimated here for $TPrA^{\bullet+}$.[32] Under some experimental conditions, such as strongly acidic solution and formation by ionizing radiation, the ESR of several small aliphatic amines cation radicals has been reported.[22,32−34]

To detect the $TPrA^{\bullet+}$ cation radicals, an ESR quartz flat flow cell was used. Such cells have proven effective in producing a steady-state concentration of many reactive intermediates within the microwave cavity of the ESR instrument. Freshly prepared $\sim$0.03 M $Ru(bpy)_3^{3+}$ and 0.10 M TPrA (pH 7) aqueous solutions were flowed into the mixing chamber at a rate of 2 to 5 mL/s and the ESR spectrum of the product in the quartz cell obtained. The major advantages of using $Ru(bpy)_3^{3+}$ as the oxidant are that the reaction between $Ru(bpy)_3^{3+}$ and TPrA is rapid at neutral pH[4] and it is a one-electron-transfer process. Many other oxidants, such as Ce^{4+}, $KMnO_4$, $KBrO_3$, and Cl_2, were found to be unsuitable for TPrA oxidation because either they required the use of strongly acidic solutions, where TPrA oxidation was slow, the oxidant itself or its reduction products gave strong ESR background, or the redox reaction was not fast enough. Figure 10 shows the experimentally measured (dotted line) as well as the simulated (solid line) ESR spectra of $TPrA^{\bullet+}$ generated in the flow cell at 20 °C. The spectrum consists of a relatively intense and sharp septet with a splitting of $\sim$20 G due to the six equivalent α-hydrogens. On the basis of the simulation, hyperfine coupling constants of 19.87 and 20.05 G for ^{14}N (1N, $I = 1$) and α-^{1}H (6H, $I = 1/2$) were evaluated. The experimental ESR spectrum had a *g*-value of 2.0038. Recently, Liu et al.[34] have reported the structure and dynamics of $TPrA^{\bullet+}$ cation radicals generated in solid $AlPO_4$-5 by ionizing radiation. Our solution-phase ESR spectrum is consistent with their solid-state ESR spectrum at 300 K.

During the ESR experiments, $Ru(bpy)_3^{3+}$ and $Ru(bpy)_3^{+}$ species can also produce signals. However, they have no effect on the ESR spectrum of $TPrA^{\bullet+}$ because the *g*-values of these two species are very different than that of $TPrA^{\bullet+}$.[35−38] No ESR signal associated with $TPrA^{\bullet}$ was observed, probably because they were oxidized by excess oxidant in the solution. Note that

(31) Smith, P. J.; Mann, C. K. *J. Org. Chem.* **1969**, *34*, 1821.
(32) Das, S.; von Sonntag, C. *Z. Naturforsch.* **1986**, *41B*, 505.
(33) Eastland, G. W.; Rao, D. N. R.; Symons, M. C. R. *J. Chem. Soc., Perkin Trans. 2* **1984**, 1551.
(34) Liu, W.; Yamanaka, S.; Shiotani, M.; Michalik, J.; Lund, A. *Phys. Chem. Chem. Phys.* **2001**, *3*, 1611.
(35) Ledney, M.; Dutta, P. K. *J. Am. Chem. Soc.* **1995**, *117*, 7687.
(36) Quayle, W. H.; Lunsford, J. H. *Inorg. Chem.* **1982**, *21*, 97.
(37) Matsuura, K.; Kevan, L. *J. Phys. Chem.* **1996**, *100*, 10 652.
(38) Matsuura, K.; Kevan, L. *Radiat. Phys. Chem.* **2001**, *62*, 399.

the expected ESR spectrum of the carbon-centered $TPrA^{\bullet}$ would be very different than the one observed.

Conclusions

The ECL emission as a function of potential for the $Ru(bpy)_3^{2+}$/TPrA system consists of two waves. The first occurs with the direct oxidation of TPrA at the electrode, and the second where $Ru(bpy)_3^{2+}$ is oxidized. In dilute $Ru(bpy)_3^{2+}$ solutions ($< \sim\mu M$) containing mM TPrA, the intensity of the first ECL wave is significant and can be larger than that for the second ECL wave. A new route for the generation of $Ru(bpy)_3^{2+*}$ at potentials of the first wave is proposed, where $TPrA^{\bullet+}$ formed during TPrA oxidation is a sufficiently stable intermediate that can oxidize $Ru(bpy)_3^{+}$ (formed from the reduction of $Ru(bpy)_3^{2+}$ by $TPrA^{\bullet}$ free radical) to give $Ru(bpy)_3^{2+*}$. On the basis of SECM−ECL experiments and digital simulation, a half-life of $\sim$0.2 ms was estimated for $TPrA^{\bullet+}$ in aqueous solution. An ESR spectrum of $TPrA^{\bullet+}$ in aqueous solution was obtained via flow mixing experiments. Fast scan CV experiments and simulations revealed that the absence of reduction wave for $TPrA^{\bullet+}$ on the reverse scan can be attributed to the cancellation of the component of current from the reduction of $TPrA^{\bullet+}$ by the anodic current contribution from the oxidation of $TPrA^{\bullet}$. These results also explain why selection of highly efficient coreactants is difficult for determination of low concentrations of Ru-label. The coreactant must form both oxidant (e.g., $TPrA^{\bullet+}$) and reductant (e.g., $TPrA^{\bullet}$) with appropriate redox potentials and lifetimes. Thus, the deprotonation rate of $TPrA^{\bullet+}$ must be just right to build up the needed concentrations of both species.

Acknowledgment. This work has been supported by grants from IGEN, MURI−DAAD 19-99-1-0207 and the Robert A. Welch Foundation.

JA027532V